

# Lawrence Berkeley National Laboratory

## Recent Work

### Title

PRODUCTION OF NOBELIUM ISOTOPES IN REACTIONS BETWEEN VARIOUS CURIUM TARGETS AND CARBON IONS

### Permalink

<https://escholarship.org/uc/item/4nf0p0p9>

### Authors

Sikkeland, Torbjorn  
Ghiorso, Albert  
Nurmia, Matti J.

### Publication Date

1967-12-01

ej. J

University of California

Ernest O. Lawrence  
Radiation Laboratory

PRODUCTION OF NOBELIUM ISOTOPES IN REACTIONS BETWEEN  
VARIOUS CURIUM TARGETS AND CARBON IONS

Torbjorn Sikkeland, Albert Ghiorso and Matti J. Nurmiä

December 1967

RECEIVED  
LAWRENCE  
RADIATION LABORATORY

LIBRARY AT  
DOCUMENTS SECTION

TWO-WEEK LOAN COPY

This is a Library Circulating Copy  
which may be borrowed for two weeks.  
For a personal retention copy, call  
Tech. Info. Division, Ext. 5545

UCRL-18011  
ej. J

## **DISCLAIMER**

This document was prepared as an account of work sponsored by the United States Government. While this document is believed to contain correct information, neither the United States Government nor any agency thereof, nor the Regents of the University of California, nor any of their employees, makes any warranty, express or implied, or assumes any legal responsibility for the accuracy, completeness, or usefulness of any information, apparatus, product, or process disclosed, or represents that its use would not infringe privately owned rights. Reference herein to any specific commercial product, process, or service by its trade name, trademark, manufacturer, or otherwise, does not necessarily constitute or imply its endorsement, recommendation, or favoring by the United States Government or any agency thereof, or the Regents of the University of California. The views and opinions of authors expressed herein do not necessarily state or reflect those of the United States Government or any agency thereof or the Regents of the University of California.

to be submitted to Physical Review

UCRL-18011  
Preprint

UNIVERSITY OF CALIFORNIA

Lawrence Radiation Laboratory  
Berkeley, California

AEC Contract No. W-7405-eng-48

PRODUCTION OF NOBELIUM ISOTOPES IN REACTIONS BETWEEN  
VARIOUS CURIUM TARGETS AND CARBON IONS

Torbjorn Sikkeland, Albert Ghiorso and Matti J. Nurmiä

December 1967

PRODUCTION OF NOBELIUM ISOTOPES IN REACTIONS BETWEEN  
VARIOUS CURIUM TARGETS AND CARBON IONS\*

Torbjorn Sikkeland, Albert Ghiorso and Matti J. Nurmiä

Lawrence Radiation Laboratory  
University of California  
Berkeley, California

December 1967

ABSTRACT

Excitation functions for the synthesis of  $^{251}\text{No}$ ,  $^{252}\text{No}$ ,  $^{253}\text{No}$ ,  $^{254}\text{No}$ ,  $^{255}\text{No}$ ,  $^{256}\text{No}$ , and  $^{257}\text{No}$  in the bombardments of  $^{244}\text{Cm}$ ,  $^{246}\text{Cm}$ , and  $^{248}\text{Cm}$  with  $^{12}\text{C}$  and  $^{13}\text{C}$  are presented. A good fit to these functions has been obtained by the use of the Jackson formula as modified to include fission and angular momentum effects. Experimental  $\overline{\Gamma_n/\Gamma_f}$  values are compared with the semi-empirical formula of Fujimoto and Yamaguchi and the following new empirical formula:  
 $\log \Gamma_n/\Gamma_f = -0.276Z + f(N)$ , where  $f(N)$  is  $5.46 + 0.140N$  for  $N \leq 153$  and  $19.23 + 0.050N$  for  $N \geq 153$ . A brief discussion of  $\Gamma_n/\Gamma_f$  systematics of trans-berkelium nuclides and the effect of the 152 neutron subshell is given.

## I INTRODUCTION

Heavy ion reactions, characterized by the formation of a compound nucleus followed by neutron emission, constitute an efficient method for the production of neutron deficient nuclides. In many cases the identification of the products is based on the analysis of their excitation functions. In regions where fission can be ignored the use of Jackson's neutron emission formula,<sup>1</sup> as modified to include angular momentum effects, has been successful in fitting the experimental functions.<sup>2</sup>

In the heavy element region fission competes strongly with neutron emission in the decay of the compound nucleus and the cross sections depend critically on the value of the ratio  $\Gamma_n/\Gamma_f$ , where  $\Gamma_n$  and  $\Gamma_f$  are the partial widths for neutron emission and fission, respectively. This ratio varies both with Z and A and a knowledge of its systematic behavior therefore is of great importance in the synthesis of the heaviest nuclides. Vandenbosch and Huizenga have made an extensive survey of experimental  $\Gamma_n/\Gamma_f$  values obtained in  $\gamma$ , n, p, d, and  $\alpha$  induced reactions.<sup>3</sup> They find such values for Pu isotopes to be fairly well reproduced by the formula of Fujimoto and Yamaguchi.<sup>4</sup>

Up to now nuclides of californium have been the heaviest ones for which an extensive set of production cross section data in heavy-ion induced reactions has been obtained and analyzed.<sup>5</sup> Again the formulas by Jackson and Fujimoto and Yamaguchi were successfully applied.

Recently, nuclides of element 102, nobelium, with mass numbers from 251 to 257, have been produced in Cm(C, xn)No reactions.<sup>6</sup> We shall in the present paper analyze the excitation functions obtained in that work. In these reactions, nuclides with neutron numbers in excess of the N = 152 neutron subshell are produced and it will be of special interest to observe the effect of that shell on the value of the ratio  $\Gamma_n/\Gamma_f$ .

## II EXPERIMENTAL

We shall only give a brief account of the experimental arrangement since a more detailed description has been reported elsewhere.<sup>6</sup> The essentially monoisotopic targets of  $^{244}\text{Cm}$ ,  $^{246}\text{Cm}$  and  $^{248}\text{Cm}$  were made by molecular deposition to a thickness of between 0.2 to 0.5 mg/cm<sup>2</sup> on about 5 mg/cm<sup>2</sup> beryllium metal. Beams of 10.4 MeV/nucleon  $^{12}\text{C}$  and  $^{13}\text{C}$  ions from the Berkeley Hilac were degraded to the desired energies by the use of Be foils. The energy spectrum of the ions leaving the target was occasionally measured by the use of a diffused-junction Si detector. The most probable energy is believed to be accurate to  $\pm 2$  MeV. The beam currents were typically  $2 \times 10^{12}$  particles/sec in an area of 0.2 cm<sup>2</sup>. Atoms recoiling from the target are stopped in a stream of helium at 600 torr and carried by this gas through an orifice about 0.2 mm in diameter into an evacuated space. The gas jet impinges a few millimeters away on the periphery of a wheel and a large fraction (~80%) of the heavy atoms attach themselves to its surface. At regular intervals the wheel is digitally rotated about 50° to expose the collected atoms to Au-Si surface barrier alpha particle detectors. In this series of experiments four detectors, equally spaced along the circumference of the wheel, were used simultaneously in order to obtain half-life information as well as alpha particle energies. Spontaneous fissions were also recorded in these experiments.

The total counting efficiency, defined as the ratio of the counts observed to the alpha disintegrations undergone by the nuclei transmuted from the target, was found experimentally to be about 10 percent. Half lives and yield of spontaneous fission activities were also measured in separate experiments in which the recoils were caught on a rotating drum in vacuum and the fission fragments were recorded by mica detectors placed along the periphery of the drum.

### III EXPERIMENTAL RESULTS

Alpha energy spectra obtained in these experiments have been given previously.<sup>6</sup> A summary of the decay characteristics of the No isotopes is given in Table I. Only about 80 events were recorded in the decay of  $^{251}\text{No}$  whereas for the other ones several hundred events were used in the half-life measurements. In the estimation of the cross sections we assumed the  $\alpha$  branching to be 100% for all isotopes except for  $^{252}\text{No}$ .

In the analysis of the  $\alpha$  spectra, a difficulty was encountered by the discovery that the 2.6-sec, 7.14-MeV  $^{214}\text{Ra}$  decayed by electron capture with a branching of  $(9.5 \pm 0.8) \times 10^{-4}$  to the 4-msec, 8.43-MeV  $^{214}\text{Fr}$ . The isotope  $^{214}\text{Ra}$  is produced from lead impurities in the targets, and in our experimental arrangement this results in an apparent 2.6-sec, 8.4-MeV  $\alpha$  activity that in some instances interfered with the radiations from  $^{252}\text{No}$  and  $^{256}\text{No}$  (see Table I). However, the number of alphas from  $^{214}\text{Fr}$  present in the observed peak at 8.4 MeV could be computed from the observed number of alphas from  $^{214}\text{Ra}$  and its EC branching. Thus, corrected half lives and cross sections for these two No isotopes could be obtained. The extent of such corrections in cross section measurements is illustrated in Fig. 1 for the systems ( $^{244}\text{Cm} + ^{12}\text{C}$ ), ( $^{248}\text{Cm} + ^{12}\text{C}$ ), and ( $^{248}\text{Cm} + ^{13}\text{C}$ ). Here the measured ratio (yield of 8.4 MeV alphas/yield of 7.14 MeV alphas) is plotted versus ion energy. For comparison the same plot for the system ( $\text{Pb}^{\text{nat}} + ^{12}\text{C}$ ) has also been included. We see that for the latter system the ratio is independent of ion energy suggesting that the 8.4 MeV alphas are coming from a daughter of the 2.6-sec, 7.14-MeV  $^{214}\text{Ra}$ . For the other systems the 8.4 MeV alphas are mostly those from  $^{214}\text{Fr}$  whereas at lower energy the ratio is substantially higher than that for Pb. The half-lives of  $^{252}\text{No}$  and  $^{256}\text{No}$  were measured at the lowest energies where the correction due to  $^{214}\text{Fr}$  was small.



The cross sections for the production of the various No isotopes are plotted versus ion energy in Figs. 2-5. To compare the cross sections for the production of the 2.5 sec SF emitter with those of the 2.5-sec, 8.4-MeV  $\alpha$  emitter, the former have been multiplied by two. The curves represent calculated values as described later under Discussion. Typical errors are indicated by error bars and are based on counting statistics only. In addition to these errors we have uncertainties and inhomogeneities in the target thicknesses and a variation and systematic errors in the collection efficiency which together might be as high as 50%.

No errors are given for the systems  $^{246}\text{Cm}(^{12}\text{C}, 4n)^{255}\text{No}$  and  $^{246}\text{Cm}(^{12}\text{C}, 5n)^{254}\text{No}$  (see Fig. 6) because of the near coincidence of the alpha energies of these two No isotopes. Consequently their yield measurements had to be based on the separation of a decay curve, consisting of only four points, into two components of similar half-lives (3 min and 1 min).

We notice (see Fig. 3) that at the highest ion energies the cross sections for the 2.5 sec SF activity, assigned to  $^{252}\text{No}$ , are relatively higher than those for the 8.4 MeV alphas from the same isotope. This may be explained by the presence of SF activity from  $^{246}\text{Fm}$  produced in a  $^{244}\text{Cm}(^{12}\text{C}, \alpha 6n)$  reaction. The half life of  $^{246}\text{Fm}$  is 1.5 sec with a SF branching of 8%<sup>7</sup> and the half-life measurements at the highest energies were not accurate enough to yield a separation of the 2.5 sec and 1.5 sec components. The assignment of the 2.5 sec SF activity to  $^{252}\text{No}$  is first of all based on the fact that its maximum production cross-section is at 73 MeV for the system  $(^{244}\text{Cm} + ^{12}\text{C})$  and 82 MeV for the system  $(^{244}\text{Cm} + ^{13}\text{C})$  (see Figs. 3 and 4).

#### IV DISCUSSION

We shall follow closely the procedure used in Ref. 5 in which a good fit to the experimental cross sections was obtained with the following formula:

$$\sigma_x(E_i) = \left\{ \prod_{i=1}^x \left[ \frac{\Gamma_n}{\Gamma_n + \Gamma_f} \right] \right\}_i \sigma_{CN} P_x \quad (1)$$

where

$$\sigma_{CN} P_x = \sum_{l=0}^{l_{CN}} \sigma_l(E_i) P_{x,l}(E)$$

Here,  $\Gamma_n$  and  $\Gamma_f$  have been defined earlier;  $E_i$  is the bombarding energy;  $\sigma_l$  is the cross section for the  $l$ -th partial wave;  $l_{CN}$  is a cut-off value at which the reactions are assumed to change from the compound nucleus type to the grazing type; and  $P_{x,l}(E)$  is the probability for the emission of exactly  $x$  neutrons from a compound nucleus of angular momentum  $l$  and excitation energy  $E$ . Formulas for  $\sigma_l$ ,  $l_{CN}$ ,  $P_{x,l}$ , and  $\Gamma_n/\Gamma_f$  shall be given later in the discussion.

Formula (1) is based on the assumption that  $\Gamma_n/\Gamma_f$  is independent of  $E_i$ , (or  $E$  and  $l$ ), and thus, that the shape of the function is determined by  $\sigma_{CN} P_x$ . The analysis is therefore performed in two steps. First, we attempt to reproduce the shape of the experimental cross section curves by adjusting a few parameters in the formula for  $P_{x,l}$  (see following Section). This will give us calculated values for  $\sigma_{CN} P_x$ . By inserting these values and experimental  $\sigma_x$  values into Eq (1), we obtain average experimental  $\overline{\Gamma_n/\Gamma_f}$  values which will be fitted to calculated ones.

#### A. The Shape of the Excitation Function

The values for the quantities,  $\sigma_l$ ,  $l_{CN}$ , and  $P_{x,l}$  in the sum term,  $\sigma_{CN} P_x$ , of Eq (1) are calculated in the following way:

1)  $\sigma_l = \pi \lambda^2 (2l+1) T_l$ , where  $\lambda$  is the reduced de Broglie wave length and  $T_l$  is the transmission coefficient for the  $l$ -th partial wave through the following potential,  $V_l(r)$ , between the interacting nuclei:<sup>8</sup>

$$V_l(r) = \frac{Z_1 Z_2 e^2}{r} + \frac{\hbar^2 l(l+1)}{2\mu r^2} + V_0 \exp \frac{r_0 (A_1^{1/3} + A_2^{1/3}) - r}{d} \quad (2)$$

where  $Z_1$  and  $A_1$  are their atomic numbers and mass numbers, respectively;  $\hbar$  is Planck's constant divided by  $2\pi$ ;  $\mu$  is the reduced mass of the system;  $V_0$ ,  $r_0$ , and  $d$  are optical model parameters for which we shall use the empirical values -70 MeV, 1.24 fm, and 0.48 fm, respectively.<sup>9</sup>

We make the approximation that  $V_\ell(r)$  at the peak is parabolic in shape and  $T_\ell$  is then given by:<sup>10</sup>

$$T_\ell = \left\{ 1 + \exp \left[ 2\pi(B - E_c) / \hbar\omega \right] \right\}^{-1}$$

Here,  $B$  is the barrier height of  $V_\ell(r)$ ,  $E_c$  is the kinetic energy of both particles in the center of mass system, and

$$\omega = \left[ -\partial^2 V / \mu \partial r^2 \right]^{1/2}$$

where  $\partial^2 V / \partial r^2$  is evaluated at the peak of  $V_\ell(r)$ , i.e., where  $\partial V / \partial r = 0$ .

2) The value of  $\ell_{CN}$  is chosen such that the ratio:

$$\frac{\sum_{\ell=0}^{\ell_{CN}} \sigma_\ell}{\sum_{\ell=0}^{\infty} \sigma_\ell}$$

(where the sums represent the cross sections for compound nucleus formation and total interaction, respectively), is equal to the experimental value of 0.8 as obtained for the system  $^{238}\text{U} + 120 \text{ MeV } ^{12}\text{C}$ .<sup>11</sup> We shall assume the value of this ratio to be independent of  $E_i$ .<sup>12</sup>

$$3) P_{x,\ell}(E) = I(\Delta_x, 2x-3) - I(\Delta_{x+1}, 2x-1)$$

where  $I(Z, n)$  is Pearson's incomplete gamma-function,

$$\Delta_x = (E - \sum_{i=1}^x B_i - E_R) / T, \text{ and } \Delta_{x+1} = (E - \sum_{i=1}^x B_i - E_{x+1}^f - E_R) / T$$

Here,  $E$  is defined above;  $B_i$  is the binding energy of the  $i$ -th neutron;  $T$  is the nuclear temperature;  $E_R$  is the rotational energy at the equilibrium configuration and shall be estimated from the formula  $E_R = (\hbar^2 / 2\mathcal{I}) \ell(\ell+1)$ , where  $\mathcal{I}$  is the effective moment of inertia; and  $E_{x+1}^f$  is the fission barrier of the product nucleus ( $E_{x+1}^f < B_{x+1}$ ).

The following assumptions are the basis for the estimation of  $P_{x, l}$ :

- (1) the nuclear temperature for neutron emission is equal to that for fission and is independent of  $E$  and  $l$ ,
- (2) the rotational energy at the equilibrium configuration is equal to that at the saddle point,
- (3) the effective moment of inertia is independent of  $E$  and  $l$ ,
- (4) rotational energy is not available for neutron emission and fission,<sup>15</sup>
- (5) angular momentum carried off by neutrons is negligible,
- (6) the angular momentum distribution does not change during the cascade and is equal to that of the compound nucleus, and
- (7) gamma emission takes place only when the excitation energy of a nucleus is less than  $(E_f + E_R)$ .

The calculation of  $\sigma_{CN} P_x$ , in 2 MeV intervals of  $E_i$ , was performed on a CDC 6600 computer. Values for  $B$  and  $E^f$  were taken from Refs. 13 and 14, respectively, and in the estimation of  $E$  we used the masses from Ref. 13. The quantities  $T$  and  $\hbar^2/2\mathcal{I}$  were the only adjustable parameters.

Best fit was obtained with  $T = 1.2 \pm 0.1$  MeV and  $\hbar^2/2\mathcal{I} = 4.5 \pm 4.5$  keV. These values are identical to those obtained in Ref. 5 for  $U(C, xn)$  systems although the errors in  $\hbar^2/2\mathcal{I}$  in the present investigations are larger since only 3, 4 and 5n reactions were involved. We notice that a fit in these cases can actually be obtained with  $\hbar^2/2\mathcal{I} = 0$ , i.e. with no rotational energy terms. In Ref. 5, where reactions involving the emission of between 3 and 8n neutrons were analyzed, it was not possible to obtain a fit with  $\hbar^2/2\mathcal{I} = 0$ . Hence, for comparison we shall in the following adopt the values  $T = 1.2$  MeV and  $\hbar^2/2\mathcal{I} = 4.5$  keV.

The results are shown in Fig. 2-7 where the curves, representing calculated values are seen to follow the experimental point quite well. The curves are normalized to the experimental points at the peak and are also shifted a certain amount  $\Delta E$

along the experimental energy scale so as to give the best fit. The values for  $\Delta E$  for the various systems are given in Table II. The average value of  $\Delta E$  is 0.2 MeV with a st. dev. of 1.5 MeV which is inside the experimental uncertainty of 2 MeV.

The effects of the energy spread of the beam on the width of the excitation functions were not taken into account. Such a correction might make the FWHM of the peaks as much as 2 MeV smaller.

## B. $\Gamma_n/\Gamma_f$ Systematics

### 1. Experimental $\Gamma_n/\Gamma_f$ Values

We define a mean value of  $\Gamma_n/\Gamma_f$  as:

$$\overline{\Gamma_n/\Gamma_f} = \bar{G}/(1-\bar{G})$$

Here  $\bar{G}$  is a mean value of  $\Gamma_n/(\Gamma_n+\Gamma_f)$  defined as:

$$\bar{G} = \left\{ \prod_{i=1}^x \left[ \Gamma_n/(\Gamma_n+\Gamma_f) \right]_i \right\}^{1/x}$$

that according to Eq (1) is given by:

$$\bar{G} = \left[ \sigma_x / (\sigma_{CN}^P x) \right]^{1/x} \quad (3)$$

Values for  $\overline{\Gamma_n/\Gamma_f}$ , estimated at the peak of  $\sigma_x$  and  $\sigma_{CN}^P$ , are listed in Table II together with the quantity  $A_{av}$  which represents the mass number of the intermediate fissioning nucleus half way along the evaporation chain. The errors for  $\overline{\Gamma_n/\Gamma_f}$  are about 50, 25 and 20% when  $\overline{\Gamma_n/\Gamma_f}$  is estimated from a  $3n$ ,  $4n$  and  $5n$  reaction, respectively. They include experimental errors in  $\sigma_x$  and uncertainties in  $\sigma_{CN}^P$  due to uncertainties of 0.02 fermis in  $r_0$  and  $d$ , 0.1 MeV in  $T$  and 4.5 keV in  $\hbar^2/2\mathcal{I}$ .

### 2. Semi-Empirical Formula for $\overline{\Gamma_n/\Gamma_f}$

We have assumed above that  $\Gamma_n/\Gamma_f$  is independent of both  $E$  and  $\ell$ . A formula for  $\overline{\Gamma_n/\Gamma_f}$  that does not contain  $E$  or  $\ell$  was developed by Fujimoto and

Yamaguchi.<sup>4</sup> Using this formula and including odd-even terms,<sup>15</sup> the geometric mean value for  $\Gamma_n/\Gamma_f$  in a cascade of  $x$  neutrons from an even  $Z$  nucleus can be written as:<sup>5</sup>

$$\overline{\Gamma_n/\Gamma_f} = c A_{av}^{2/3} \exp(\beta\Delta/x) \exp \left\{ \left[ \sum_{i=1}^x (E_i^f - B_i) \right] / xT \right\} \quad (4)$$

where  $A_{av}$ ,  $E_i^f$ ,  $B_i$ , and  $T$  have been defined earlier;  $e$  and  $\Delta$  are constants; and

$$\beta = \begin{cases} 0, & n_{ee} = n_{eo} \\ 1, & n_{ee} > n_{eo} \\ -1, & n_{ee} < n_{eo} \end{cases} \quad (n_{ee} \text{ and } n_{eo} \text{ are the numbers of even-even and even-odd nuclides in the cascade, respectively})$$

This formula which is a good approximation for  $E - B_i \geq 3 \text{ MeV}$ <sup>15</sup> is based on the constant temperature level density formula<sup>15</sup> (as is the formula for  $P_{x,\ell}$ ) and on the assumption that pairing energies only depend on the even or odd characters of  $Z$  and  $N$ .

Values for  $\overline{\Gamma_n/\Gamma_f}$  calculated according to this formula were now fitted to the experimental ones by adjusting the constants,  $c$ ,  $\Delta$ , and  $T$ , and using the values for  $B$  and  $E^f$  from Refs. 13 and 14, respectively. Best fit was obtained with  $c=0.63$ ,  $\Delta=1.4$ , and  $T=0.6 \text{ MeV}$  which reproduced the experimental values with a st. dev. of 22%. Calculated  $\overline{\Gamma_n/\Gamma_f}$  values are compared to the experimental ones in Table II.

When only  $4n$  and  $5n$  cross sections are considered the experimental values are reproduced with a st. dev. of 10%. This is a factor of two better than the estimated experimental errors. The reason for this is that the calculated values are normalized to the experimental ones and hence, systematic experimental errors are eliminated.

A closer examination of the experimental and calculated  $\overline{\Gamma_n/\Gamma_f}$  values in Table II reveals that for  $3n$  reactions the former are systematically and on the average 30% lower than the latter. This discrepancy can be removed by using

a value of 1.1 MeV instead of 1.2 MeV for the nuclear temperature in the estimation of  $\sigma_{CN}^P$ . This will increase the experimental  $\overline{\Gamma}_n/\overline{\Gamma}_f$  values for the 3n reactions by 30% whereas those for the 4n and 5n reactions are practically unchanged. The values of the other parameters,  $r_0$ ,  $d$ ,  $V_0$ , and  $\hbar^2/2\mathcal{E}$  have little influence on the relative values of  $\overline{\Gamma}_n/\overline{\Gamma}_f$ . We may therefore conclude that  $\overline{\Gamma}_n/\overline{\Gamma}_f$  within experimental errors is independent of bombarding energy. This is in agreement with the conclusion drawn in Ref. 5 on the basis of a similar analysis of reactions involving the emission of between 3 and 8 neutrons.

The values for  $c$ ,  $\Delta$ , and  $T$  obtained in Ref. 5, where  $\overline{\Gamma}_n/\overline{\Gamma}_f$  for Cf isotopes were analyzed, were 0.33, 1.5, and 0.59 MeV, respectively. The large difference between the  $c$  values from these two sets of experiments is significant. This disparity is regarded as outside experimental errors. Rather we think it is in large part due to uncertainties in the values of  $E^f$  used. We find a value of 0.5 for  $c$  if we assume that the  $E^f$  values for the Cf isotopes are systematically 0.2 MeV too high and those for No isotopes 0.2 MeV too low. By extending these calculations to lighter actinides the discrepancies became even larger. For instance, to obtain a fit to experimental  $\overline{\Gamma}_n/\overline{\Gamma}_f$  values for uranium isotopes the  $E^f$  values from Ref. 14 have to be decreased by about 0.8 MeV. This suggests either some systematic and primarily Z-dependent deviations in these values or a break-down of Eq (4).

### 3. Empirical Formula for $\overline{\Gamma}_n/\overline{\Gamma}_f$

The systematic variation of  $\overline{\Gamma}_n/\overline{\Gamma}_f$  with  $N$  is illustrated in Fig. 8 for trans-berkelium nuclei of even  $Z$ . Here, the points represent experimental  $\overline{\Gamma}_n/\overline{\Gamma}_f$  values and the solid and broken lines, that connect individual  $\overline{\Gamma}_n/\overline{\Gamma}_f$  values for nuclides of the same element, represent respectively, Eq (3) with

$x=1$ ,  $c=0.5$ ,  $T=0.59$  MeV and  $\Delta=1.5$ , and the following empirical equation

$$\log \Gamma_n / \Gamma_f = -0.276 Z + \begin{cases} 5.46 + 0.140N, & \text{for } N \leq 153 \\ 19.23 + 0.050N, & \text{for } N \geq 153 \end{cases} \quad (5)$$

We see that the empirical equation gives a better overall fit. In fact, we find that Eq (5) reproduces well all the experimental  $\Gamma_n / \Gamma_f$  values for even Z trans-thorium nuclides. (A similar good fit for odd Z nuclides is obtained by adding 0.12 to the right side of Eq (5)). Hence, such a formula is more realistic to use in cross section calculations in the vicinity of nuclei for which  $\Gamma_n / \Gamma_f$  values are known.

This very nearly linear relationship between  $\log \Gamma_n / \Gamma_f$  and N, or A, below the N=152 subshell has been pointed out by several authors.<sup>15</sup> It is interesting to note that the data from the No isotopes presented here suggest a similar but less steep relationship above that shell. Such a trend is also reproduced by Eq (4) in conjunction with  $E^f$  and B values from Refs. 13 and 14.

Using Eq(4) in conjunction with Cameron's values for B and his shell and pairing corrections<sup>16</sup> for the estimation of  $E^f$  it was predicted in Ref. 17 that  $\log \Gamma_n / \Gamma_f$  in the region of the 152 shell is almost symmetric with respect to N=153, i.e. that  $\log \Gamma_n / \Gamma_f$  decreases almost as fast with N above N=153 as it increases with N below that neutron number. The fit to experimental data was good below N=153. This suggests therefore that above N=153 Cameron's values do not reproduce the systematic trend as well as do those from Ref. 13 and 14.

The three experimental points given for element 104 represent  $\Gamma_n / \Gamma_f$  values estimated from the experimental cross section<sup>18</sup> for the production of a 0.3 sec SF emitter in the reaction between  $^{242}\text{Pu}$  and  $^{22}\text{Ne}$  assuming a 3n, 4n and 5n reaction, respectively. Comparison with the extrapolated  $\Gamma_n / \Gamma_f$  values using both Eq (3) and Eq (4) suggests the 3n and 5n reactions to be the most likely candidates. In the latter case this emitter is  $^{259}_{104}$  which also



should be produced in a  $^{242}\text{Pu}(^{20}\text{Ne}, 3n)$  reaction. Since this was shown experimentally not to be the case<sup>16</sup> one may conclude that this activity is more likely due to  $^{261}_{104}$  rather than  $^{260}_{104}$  as implied in Ref. 16. However, the  $\Gamma_n/\Gamma_f$  systematics are of course too uncertain to make this isotope assignment definite.

#### V. CONCLUSION

The shapes of the experimental excitation functions are successfully reproduced by the calculated curves and such curves can therefore be used in mass assignments. To predict values of the absolute cross sections it appears, at the present time, more realistic to use an empirical formula for  $\Gamma_n/\Gamma_f$ , such as Eq (5). In using the Fujimoto-Yamaguchi formula, (Eq (4)), one has to rely on rather questionable values for the fission barrier and the neutron binding energy. Here an uncertainty of only 0.2 MeV in the quantity  $(E_f - B_n)$  will introduce an error of about 40% in the value of  $\Gamma_n/\Gamma_f$ . This error corresponds to an uncertainty of a factor of three in the predicted value for a  $4n$  cross section in a region where  $\Gamma_n/\Gamma_f$  is about 0.1. One might therefore suggest a reverse procedure namely to use Eq (4) in conjunction with experimental  $\overline{\Gamma_n/\Gamma_f}$  values to obtain "experimental" values for  $(E_f - B_n)$ .

\*This work was done under the auspices of the U.S. Atomic Energy Commission.

1. J. D. Jackson, *Can. J. Phys.* 34, 767 (1956).
2. T. Sikkeland, *Proc. of the Lysekil Symposium, 1966*, *Arkiv för Fysik*, Bd 36 nr 62, 539 (1967).
3. R. Vandenbosch and J. R. Huizenga, *Proceedings of the Second United Nations International Conference on the Peaceful Uses of Atomic Energy, 1958* (United Nations, New York, 1958) 15, P/688.
4. Y. Fujimoto and Y. Yamaguchi, *Prog. Theor. Phys.* 5, 76 (1950).
5. T. Sikkeland, J. Maly, and D. F. Lebeck, Lawrence Radiation Laboratory Report UCRL-17588, *Phys. Rev.* to be published.
6. A. Ghiorso, T. Sikkeland, M. J. Nurmia, *Phys. Rev. Lett.* 18, 401 (1967).
7. M. J. Nurmia, T. Sikkeland, R. Silva and A. Ghiorso, *Physics Letters*, 26B, 78 (1967).
8. R. D. Woods and D. S. Saxon, *Phys. Rev.* 95, 577 (1954).
9. V. E. Viola, Jr., and T. Sikkeland, *Phys. Rev.* 28, 767 (1962).
10. D. L. Hill and J. A. Wheeler, *Phys. Rev.* 89, 1102 (1952).
11. T. Sikkeland, and V. E. Viola, Jr., in *Proc. Third Conf. on Reactions between Complex Nuclei, Asilomar, April 14-18, 1963* (University of California Press, Berkeley 1963).
12. T. Sikkeland, *Phys. Rev.* 135, B669 (1964).
13. V. E. Viola, Jr., and G. T. Seaborg, *J. Inorg. Nucl. Chem* 28, 698 (1966).
14. V. E. Viola, Jr.; and B. D. Wilkins, *Nuclear Phys.* 82, 65 (1966).
15. J. R. Huizenga and R. Vandenbosch, in *Nuclear Reactions*, ed. by P. M. Endt and P. B. Smith (North-Holland Publishing Company, Amsterdam, 1962).
16. A. G. W. Cameron, *Can. J. Phys.* 35, 1021 (1957).
17. T. Sikkeland, Lawrence Radiation Laboratory Report UCRL-16348, Aug. 1965 (unpublished).
18. G. N. Flerov, Yu. Ts. Oganessian, Yu. V. Lobanov, et al., *Atomnaya Energiya*, 17, 310 (1964).  
[English transl.: *Soviet Atomic Energy*, 17, 1046 (1964).]

Table I. Decay Properties of Various  
Isotopes of Element 102.

Isotopes	Half-life (sec)	$E_{\alpha}$ (MeV) $\pm 0.02$	SF/ $\alpha$ ratio
$^{251}_{102}$	$0.8 \pm 0.3$	8.60(80%) 8.68(20%)	1/2
$^{252}_{102}$	$2.5 \pm 0.3$	8.41	
$^{253}_{102}$	$105 \pm 15$	8.01	
$^{254}_{102}$	$55 \pm 5$	8.10	
$^{255}_{102}$	$185 \pm 15$	8.11	
$^{256}_{102}$	$2.8 \pm 0.3$	8.43	
$^{257}_{102}$	$23 \pm 3$	8.23(50%) 8.27(50%)	

Table II. Results of the analysis of experimental excitation functions for Cm(C, xn) No reactions. Here,  $\sigma_{x,m}$  represents the maximum cross section and  $E_{i,m}$  the corresponding ion energy in the laboratory system as read off the curves in Figs. 2-7;  $\Delta E$  gives the amount we have shifted the calculated curves in the Figs. along the experimental energy scale to obtain a fit;  $(\sigma_{CN}^P)_m$  is the calculated maximum cross section for a (C,xn) reaction when fission competition is ignored;  $A_{av}$  represents the mass number of the intermediate fissioning nucleus half way along the evaporation chain. In the last three columns of the Table experimental  $\bar{\Gamma}_n/\bar{\Gamma}_f$  values are compared with values calculated from Eq (4) and with those obtained from Eq (5).

System	x	$E_{i,m}$ (MeV)	$\Delta E$ (MeV)	$\sigma_{x,m}$ ( $\mu$ b)	$(\sigma_{CN}^P)_m$ (mb)	$A_{av}$	$\bar{\Gamma}_n/\bar{\Gamma}_f$ (exp)	$\bar{\Gamma}_n/\bar{\Gamma}_f$ Eq (4)	$\bar{\Gamma}_n/\bar{\Gamma}_f$ Eq (5)
$^{244}\text{Cm} + ^{12}\text{C}$	4	73.3	0	0.25*	90	254.5	0.054	0.039	0.043
	5	83.0	-2	0.090	330	254	0.051	0.033	0.037
$^{244}\text{Cm} + ^{13}\text{C}$	3	69.8	0	0.12	0.8	256	0.056	0.063	0.060
	4	72.8	0	0.30	77	255.5	0.046	0.052	0.054
	5	82.0	-2	0.16*	250	255	0.061	0.053	0.047
$^{246}\text{Cm} + ^{12}\text{C}$	4	72.0	0	1.0	50	256.5	0.072	0.063	0.064
	5	83.0	-3	0.24	290	256	0.065	0.053	0.058
$^{246}\text{Cm} + ^{13}\text{C}$	3	67.5	2	0.07	0.60	258	0.051	0.083	0.076
	4	69.5	2	0.62	43	257.5	0.065	0.071	0.072
	5	78.5	2	0.56	430	257	0.071	0.071	0.068
$^{248}\text{Cm} + ^{12}\text{C}$	3	69.2	0	0.16	0.70	259	0.065	0.073	0.085
	4	71.2	0	1.0	26	258.5	0.085	0.076	0.080
	5	77.8	0	0.58	240	258	0.081	0.069	0.076
$^{248}\text{Cm} + ^{13}\text{C}$	4	70.5	1	1.1	30	259.5	0.084	0.087	0.090
	5	74.8	1	0.66	150	259	0.093	0.081	0.085

\* The combined cross sections for the 2.5 sec 8.4 MeV  $\alpha$  emitter and the 2.5 sec SF emitter.

Fig. 1. Ratio between the yield of 8.4 MeV  $\alpha$  to that of 7.14 MeV  $\alpha$  in units of  $10^{-3}$  measured as a function of ion energy for the systems  $\text{Pb}^{\text{nat}} + \text{C}$ , ( $\odot$ );  $^{244}\text{Cm} + ^{12}\text{C}$ , ( $\Delta$ );  $^{248}\text{Cm} + ^{12}\text{C}$ , ( $\circ$ ); and  $^{248}\text{Cm} + ^{13}\text{C}$ , ( $\square$ ). The ordinate scale on the left hand is for the first three systems and that on the right is for  $^{248}\text{Cm} + ^{13}\text{C}$ .

Fig. 2. Experimental cross sections plotted versus ion energy for  $^{244}\text{Cm} (^{12}\text{C}, \text{xn})^{256-x}\text{No}$  reactions. The open squares, solid squares, and circles correspond to  $x=4$  ( $\alpha$  emitter),  $x=4$  (SF emitter), and  $x=5$ , respectively.

The yields of the SF emitter have been multiplied by two. The curves represent the function  $\sigma_{\text{CN}}^{\text{P}}/x$  normalized at the peak to the experimental points. The energy scales for the curves are displaced  $\Delta E$  MeV relative to that of the points. Values for  $\Delta E$  are given in Table II.

Fig. 3. Experimental cross sections plotted versus ion energy for  $^{244}\text{Cm} (^{13}\text{C}, \text{xn})^{256-x}\text{No}$  reactions. The triangles, squares, open circles, and closed circles corresponding to  $x=3$ ,  $x=4$ ,  $x=5$  ( $\alpha$  emitter), and  $x=5$  (SF emitter), respectively. The yields of the SF emitter have been multiplied by two. The curves represent the function  $\sigma_{\text{CN}}^{\text{P}}/x$  normalized as explained in the caption for Fig. 2.

Fig. 4. Experimental cross sections plotted versus ion energy for  $^{246}\text{Cm} (^{12}\text{C}, \text{xn})^{258-x}\text{No}$ . The squares and circles correspond to  $x=4$  and  $x=5$ , respectively. The curves represent the function  $\sigma_{\text{CN}}^{\text{P}}/x$  normalized as explained in caption for Fig. 2.

Fig. 5. Experimental cross sections plotted versus ion energy for  $^{246}\text{Cm} (^{13}\text{C}, \text{xn})^{258-x}\text{No}$ . The triangles, squares, and circles correspond to  $x=3$ ,  $x=4$ , and  $x=5$ , respectively. The curves represent the function  $\sigma_{\text{CN}}^{\text{P}}/x$  normalized as explained in the caption for Fig. 2.

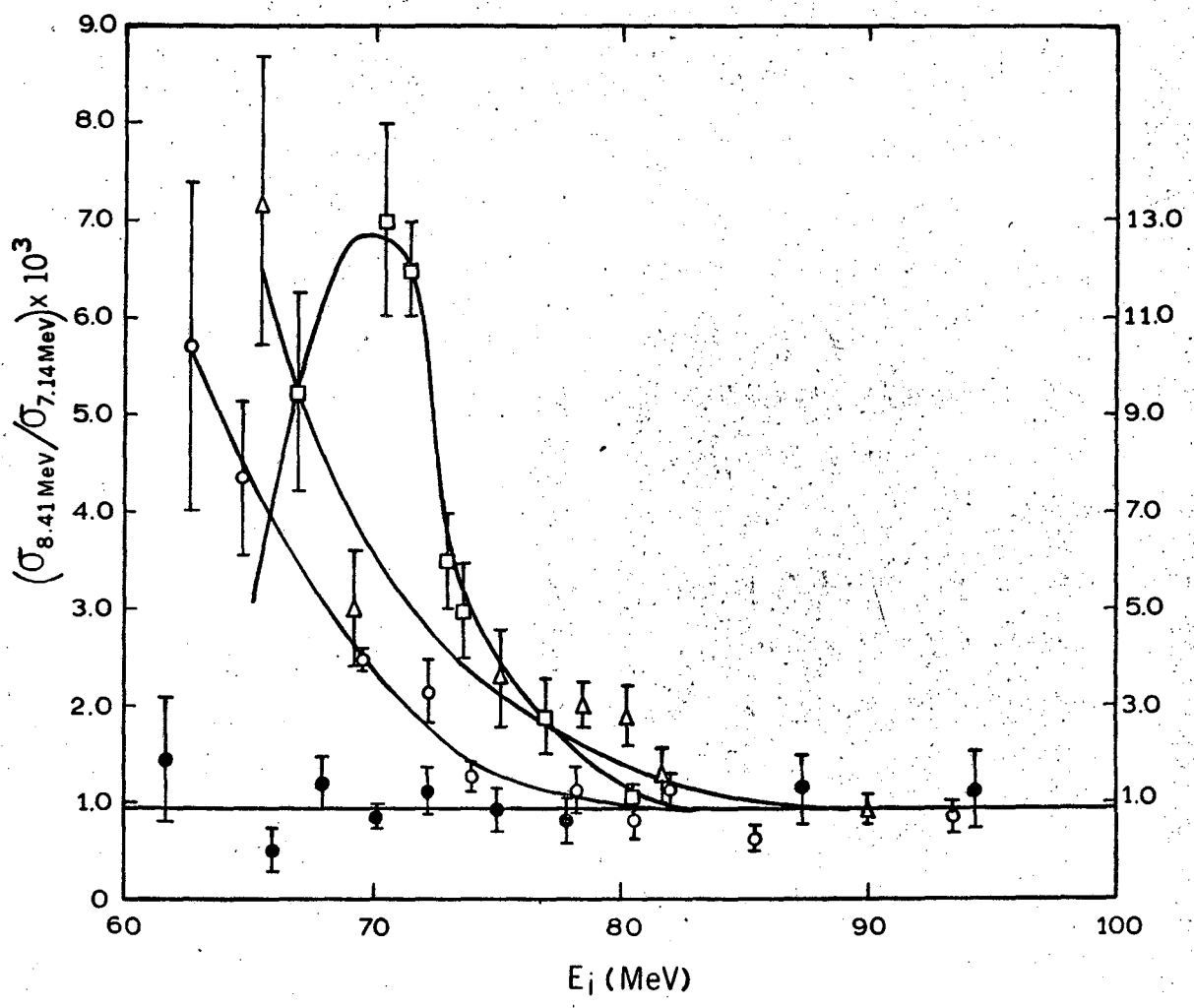
Fig. 6. Experimental cross sections plotted versus ion energy for  $^{248}\text{Cm} (^{12}\text{C}, \text{xn})^{260-x}\text{No}$ . The triangles, squares, and circles correspond to

$x=3$ ,  $x=4$ , and  $x=5$ , respectively. The curves represent the function  $\sigma_{CN}^P x$  normalized as explained in the caption for Fig. 2.

Fig. 7. Experimental cross sections plotted versus ion energy for  $^{248}\text{Cm}(^{13}\text{C}, xn)^{261-x}\text{No}$ . The squares and circles correspond to  $x=4$  and  $x=5$ , respectively. The curves represent the function  $\sigma_{CN}^P x$  normalized as explained in the caption for Fig. 2.

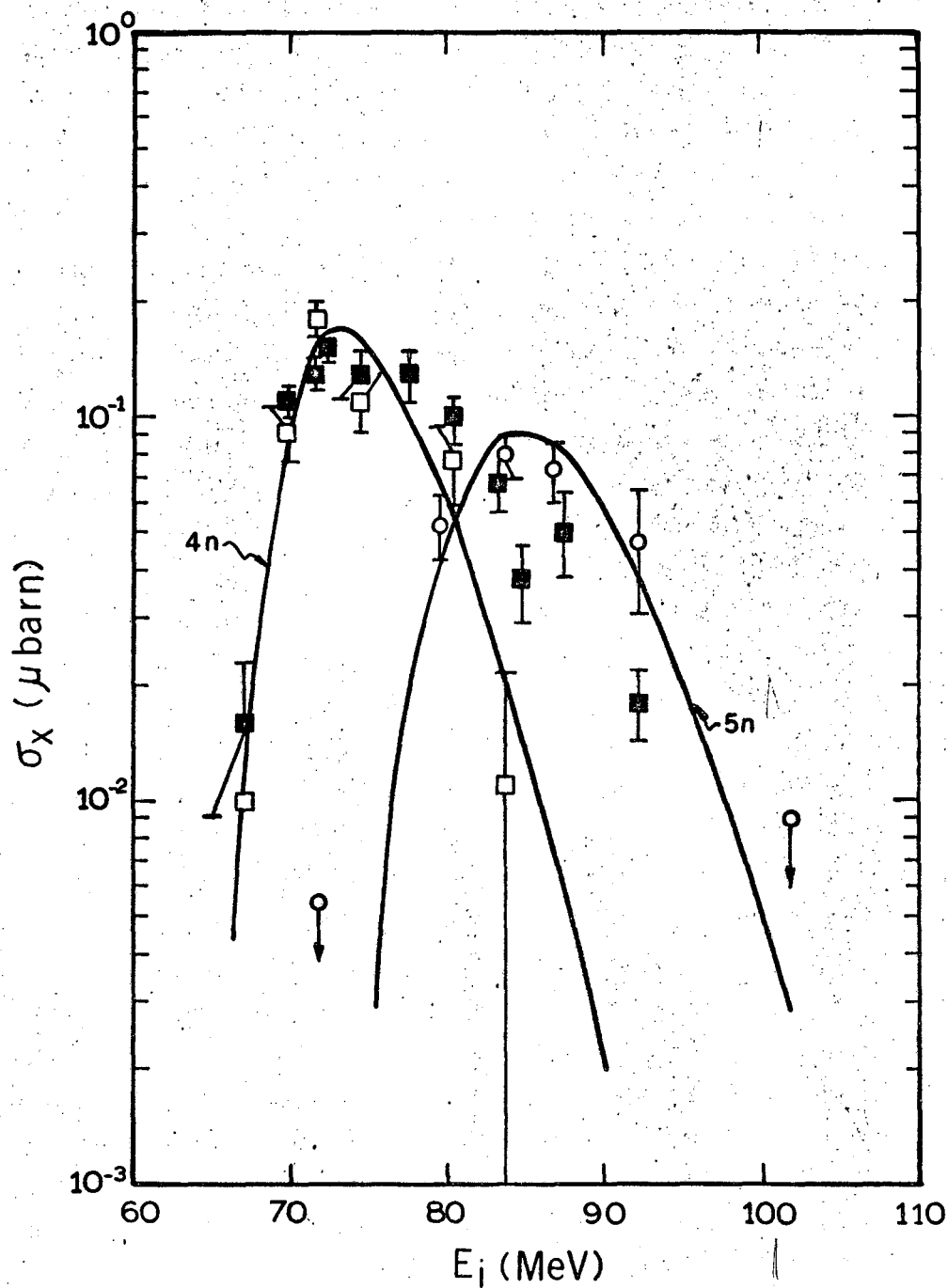
Fig. 8. Experimental  $\Gamma_n/\Gamma_f$  values for even  $Z$  trans-berkelium nuclides plotted versus the neutron number of the intermediate nucleus in the neutron cascade. The data are from the present work, from Ref. 5, and from Ref. 17. The circles, triangles, and squares represent data for Cf, Fm, and No, respectively. For element 104 we have indicated three possible values for  $\Gamma_n/\Gamma_f$  based on the assumptions that the SF emitter observed in the reaction between  $^{242}\text{Pu}$  and  $^{22}\text{Ne}^{18}$  is produced in a  $3n$  (solid triangle),  $4n$  (solid square), and  $5n$  (pentagon) reaction, respectively.

The solid lines connect individual  $\Gamma_n/\Gamma_f$  values calculated from Eq (4) as explained in the text; and the broken lines represent the empirical relationship of Eq (5).



XBL 682 4498

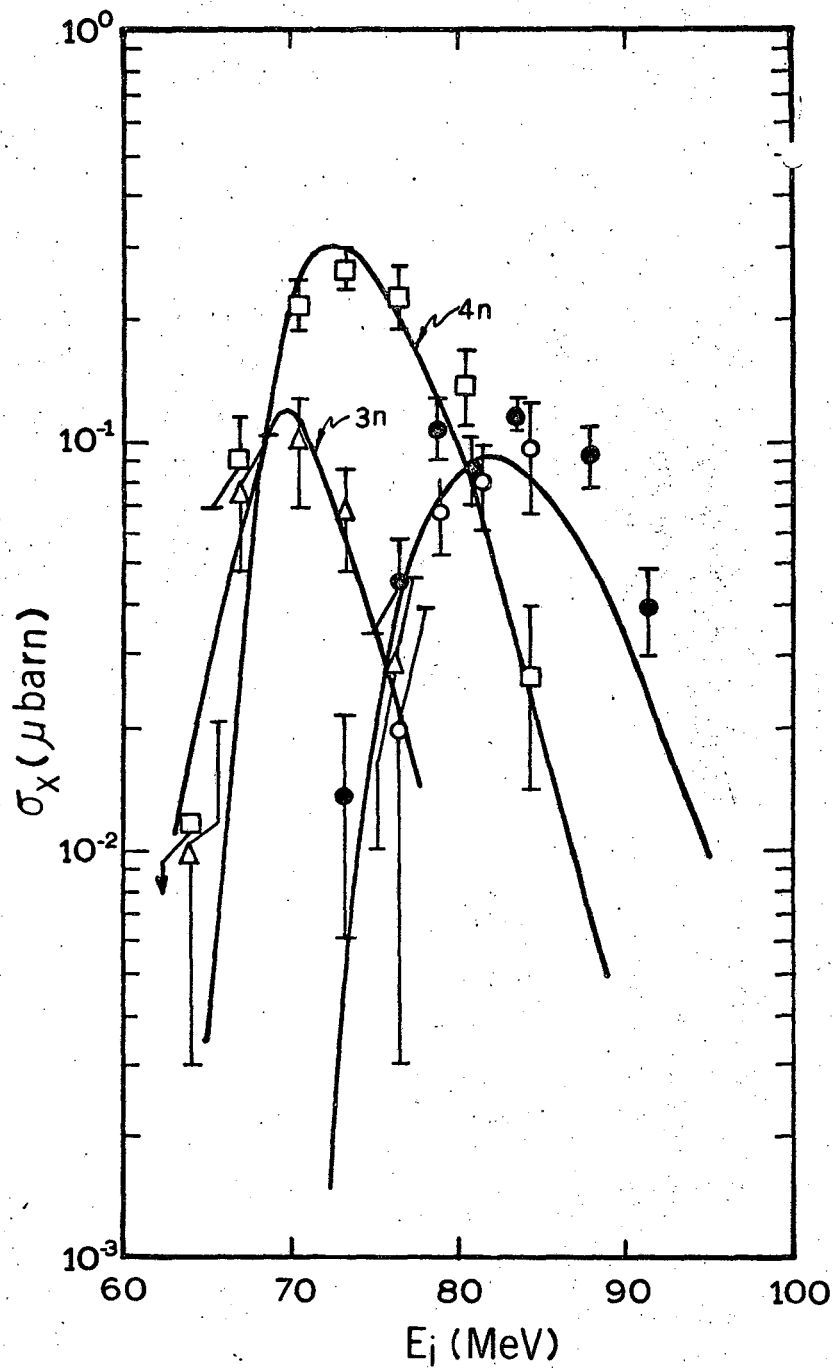
Fig. 1



XBL 682 4499

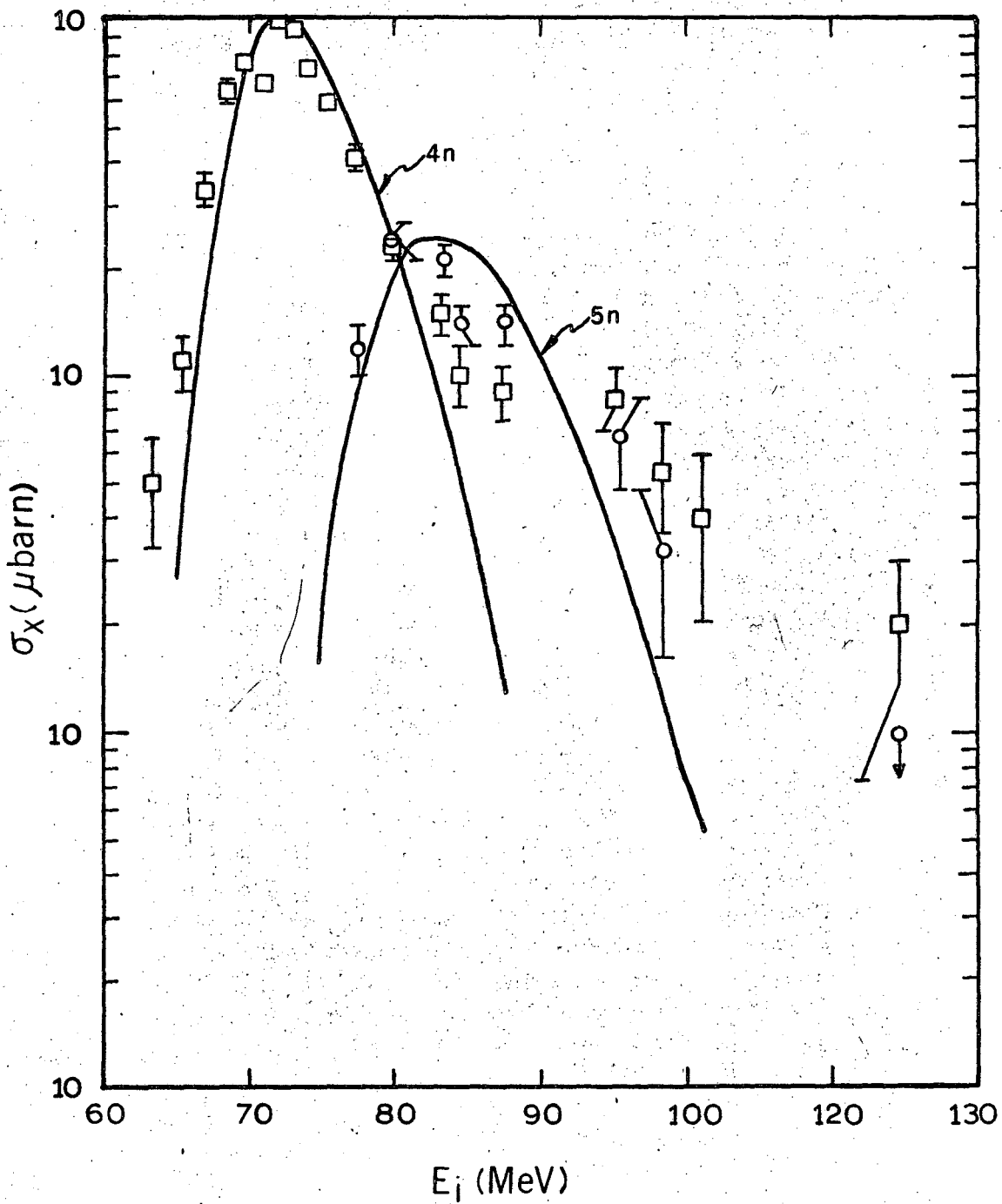
Fig. 2





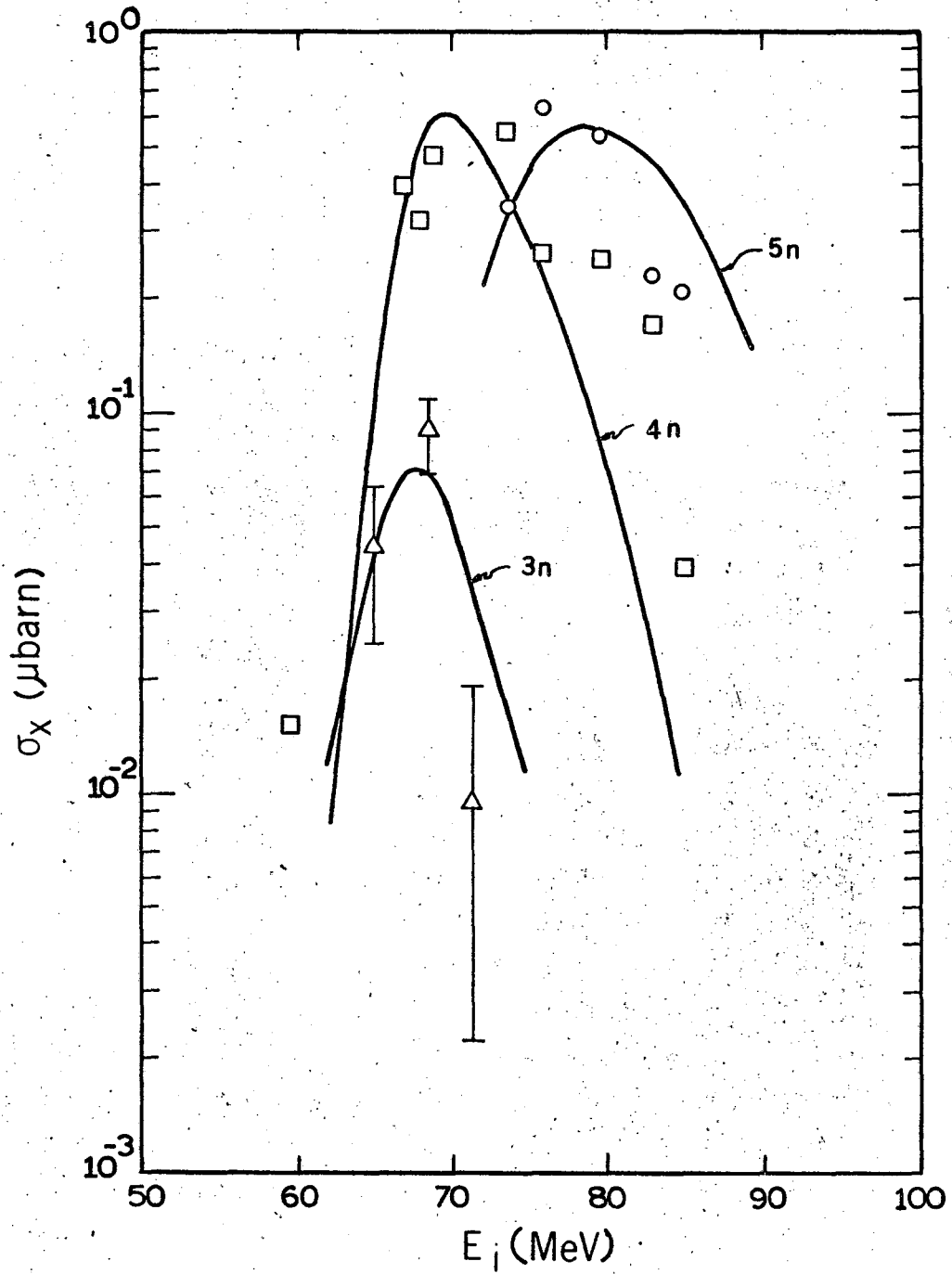
XBL 682 4500

Fig. 3



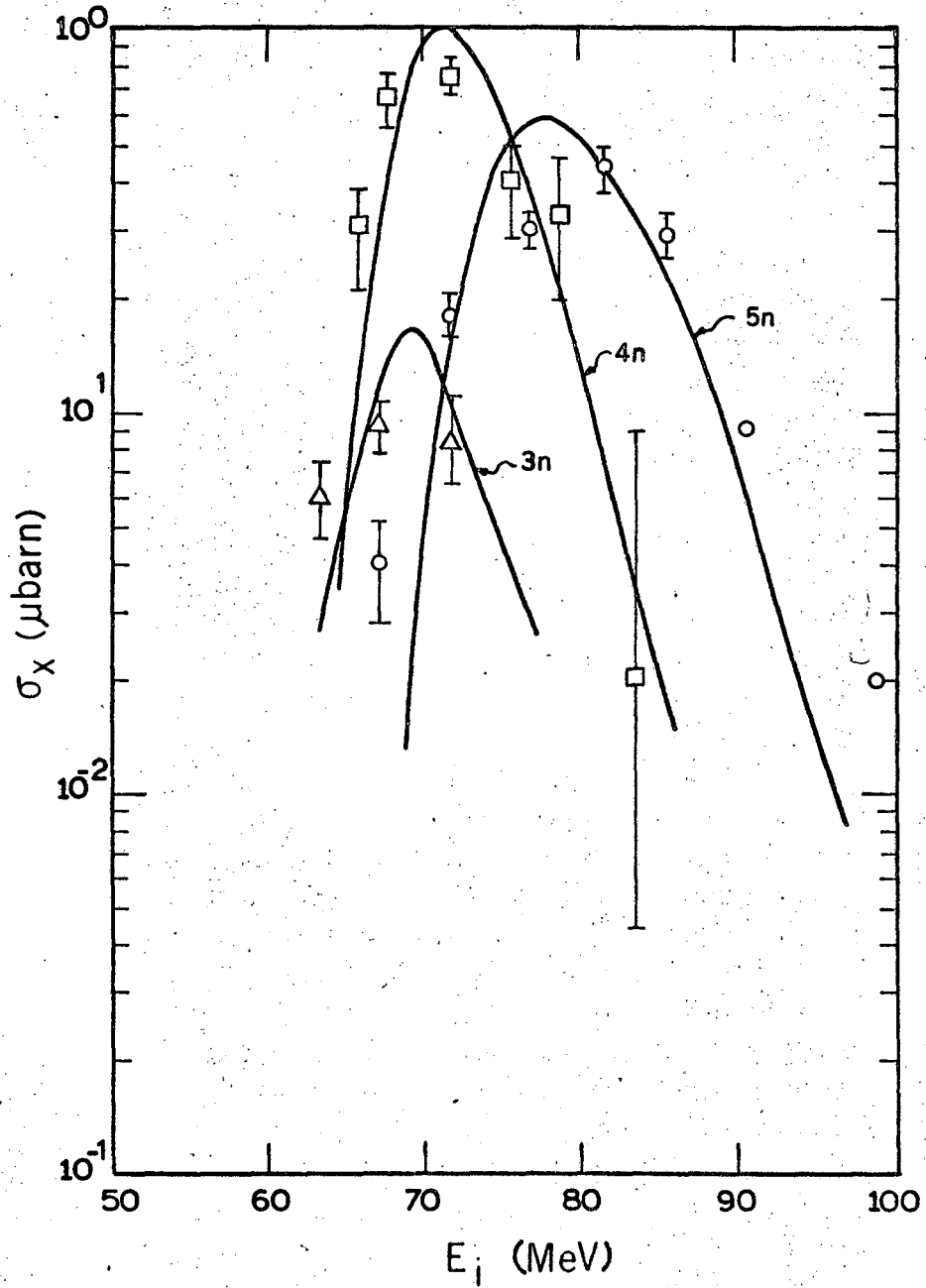
XBL 682 4801

Fig. 4



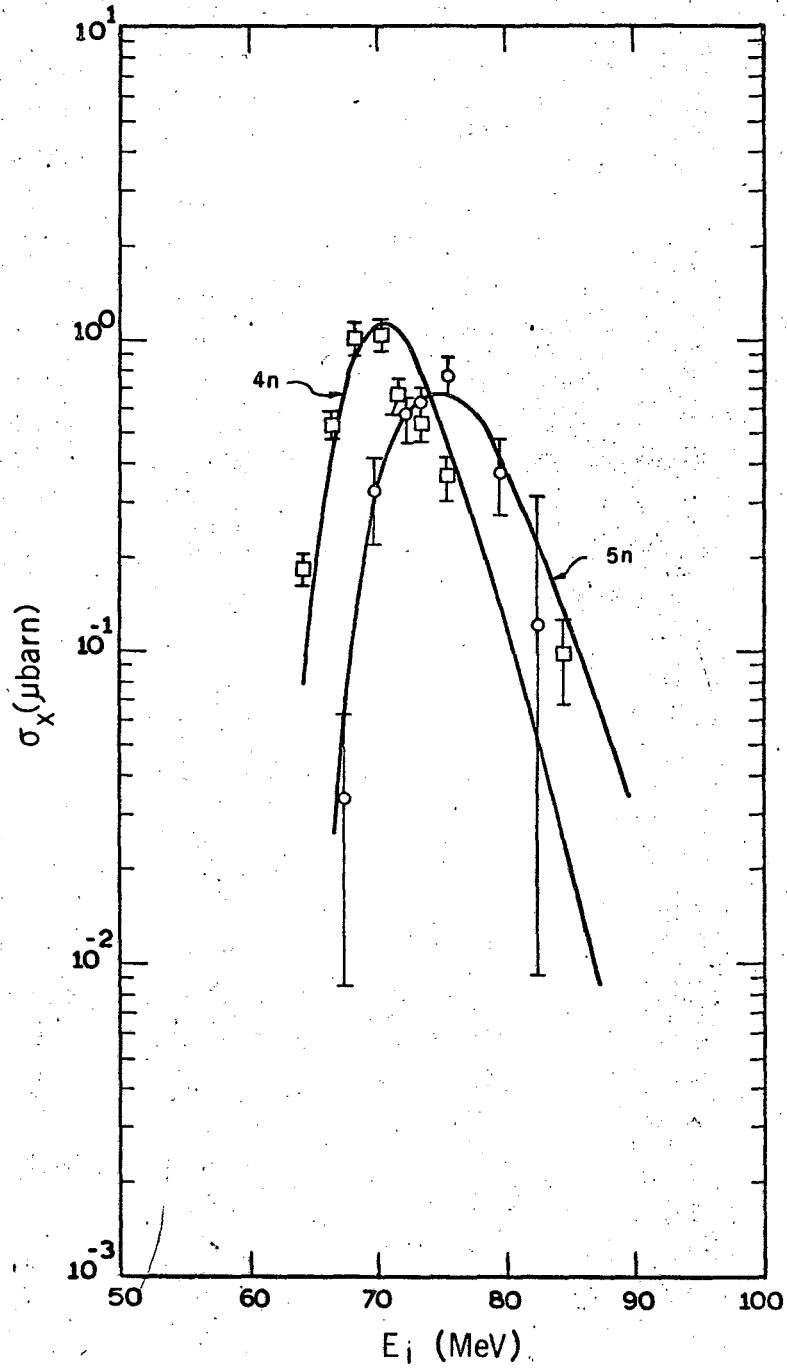
XBL 682 4802

Fig. 5



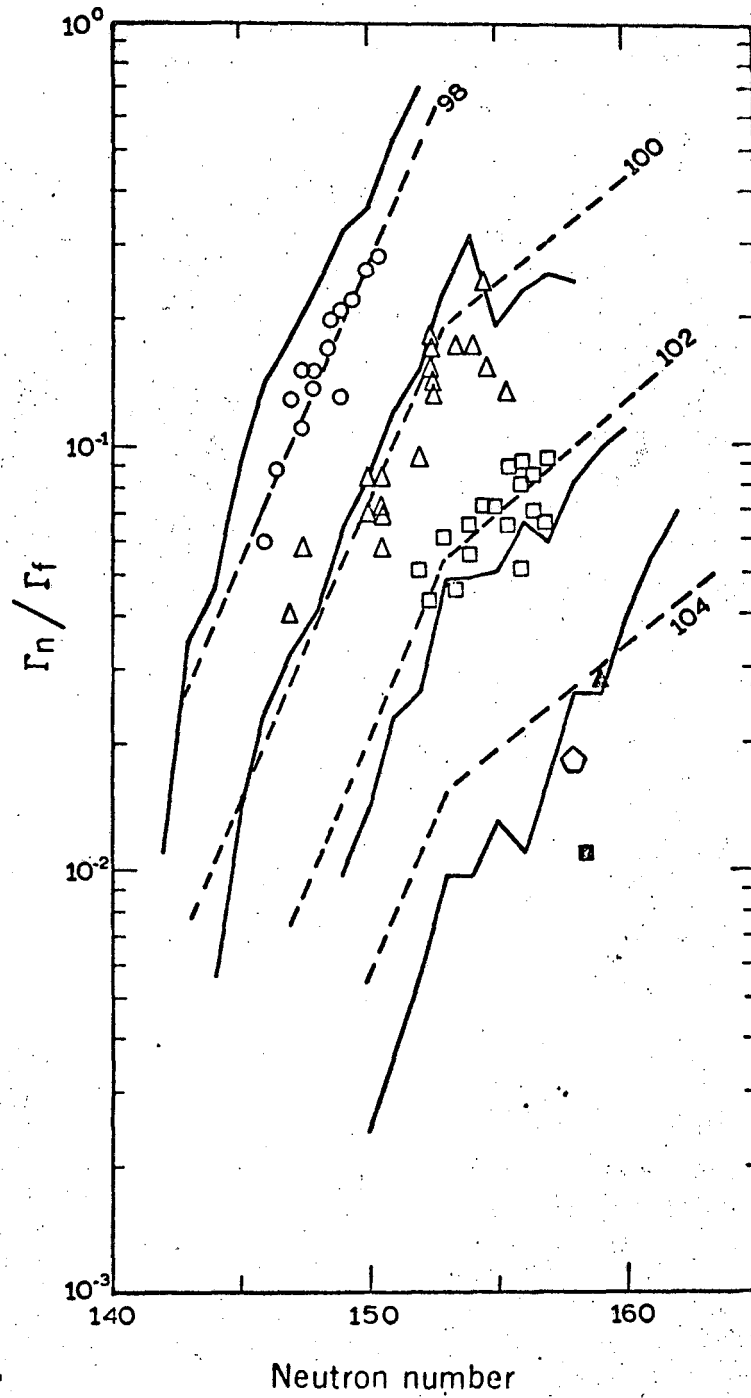
XBL 682 4803

Fig. 6



XBL 682 4804

Fig. 7



XBL682 4805

Fig. 8

This report was prepared as an account of Government sponsored work. Neither the United States, nor the Commission, nor any person acting on behalf of the Commission:

- A. Makes any warranty or representation, expressed or implied, with respect to the accuracy, completeness, or usefulness of the information contained in this report, or that the use of any information, apparatus, method, or process disclosed in this report may not infringe privately owned rights; or
- B. Assumes any liabilities with respect to the use of, or for damages resulting from the use of any information, apparatus, method, or process disclosed in this report.

As used in the above, "person acting on behalf of the Commission" includes any employee or contractor of the Commission, or employee of such contractor, to the extent that such employee or contractor of the Commission, or employee of such contractor prepares, disseminates, or provides access to, any information pursuant to his employment or contract with the Commission, or his employment with such contractor.

